

Magnetic structures of DyCo_2Si_2 and DyCu_2Si_2 : A neutron-diffraction study

H. Pinto and M. Melamud

Nuclear Research Center—Negev, P.O.B. 9001, Beer Sheva, Israel

J. Gal and H. Shaked

*Nuclear Research Center—Negev, P.O.B. 9001, Beer Sheva, Israel
and Ben-Gurion University of the Negev, P.O.B. 653, Beer Sheva, Israel*

G. M. Kalvius

*Technische Universitat, Munchen, E-15 Physik Department, 8046-D, Garching bei Munchen,
Federal Republic of Germany*

(Received 14 May 1982)

The compounds DyCo_2Si_2 and DyCu_2Si_2 were studied by neutron diffraction. The diffraction patterns of these compounds at 300 K agree with the reported crystallographic structures (space group $I4/mmm$). The diffraction pattern of DyCo_2Si_2 at 4.2 K is consistent with a type-I antiferromagnetic structure on the Dy sublattice. The magnetic moment, $(9.5 \pm 0.5)\mu_B$, lies along the c axis. The diffraction pattern of DyCu_2Si_2 at 4.2 K revealed the existence of superlattice lines consistent with a cell doubled in the a and c directions. The magnetic structure consists of ferromagnetic (101) planes of Dy coupled antiferromagnetically. The magnetic moment $(8.3 \pm 0.4)\mu_B$ lies along the b axis. The transition temperatures T_N deduced from the intensity-versus-temperature measurements of the reflections $\{010\}$ and $\{\frac{1}{2}0\frac{1}{2}\}$ for DyCo_2Si_2 and DyCu_2Si_2 , respectively, are 21 ± 2 and 11 ± 1 K. It is found that $H_{\text{eff}}(\text{kOe}) \sim 600\mu(\mu_B)$, where H_{eff} is the effective magnetic hyperfine field observed in the Mössbauer effect in ^{161}Dy (26-keV γ rays) and μ is the ordered magnetic moment observed in the neutron diffraction.

I. INTRODUCTION

The family of compounds RM_2X_2 (R =lanthanide, actinide, M =transition metal, X =Ge, Si) crystallizes in the BaAl_4 -type structure.¹⁻⁴ The structure belongs to the space group $I4/mmm-D_{4h}^{17}$ with R , M , and X at $2a$, $4d$, and $4e$ positions, respectively. This family of compounds exhibits a large variety of magnetic structures and properties. Ferromagnetic, commensurate and noncommensurate antiferromagnetic structures associated with first- and second-order phase transitions were reported.⁵⁻¹³ In all these structures magnetic ordering was found on the R sublattice and no magnetic ordering was found on the M sublattice, except in the $M=\text{Mn}$ compounds.¹⁴ In the present investigation we note the following: (i) Two commensurate antiferromagnetic structures are found, with $\vec{k}=(0,0,2\pi/c)$ in DyCo_2Si_2 and with $\vec{k}=(\pi/a,0,\pi/c)$ in DyCu_2Si_2 . (ii) The relation between the ordered magnetic moment (neutron diffraction) and the effective magnetic hyperfine field at the Dy nucleus (Mössbauer effect) is determined.

II. EXPERIMENTAL

Powder samples of DyCo_2Si_2 and DyCu_2Si_2 were synthesized by arc melting under argon atmosphere. Neutron- ($\lambda \sim 2.4 \text{ \AA}$) diffraction patterns of the two

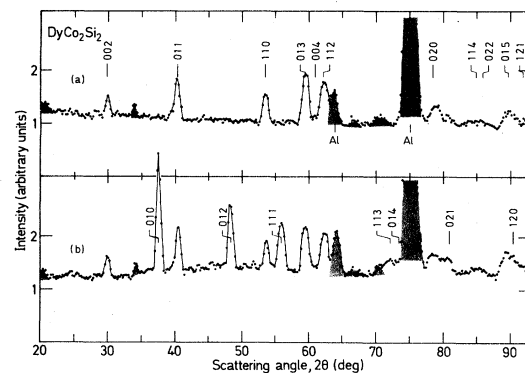


FIG. 1. Neutron ($\lambda \sim 2.45 \text{ \AA}$) diffraction patterns of DyCo_2Si_2 at (a) 300 K and (b) 4.2 K. No reflection was observed in the range $10^\circ < 2\theta < 20^\circ$ (not shown). The shaded regions contain contributions from impurities.

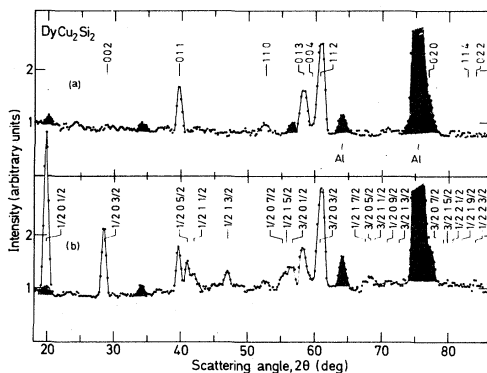


FIG. 2. Neutron- ($\lambda \sim 2.45 \text{ \AA}$) diffraction patterns of DyCu₂Si₂ at (a) 300 K and (b) 4.2 K. No reflection was observed in the range $3^\circ < 2\theta < 18^\circ$ (not shown). The shaded regions contain contribution from impurities.

compounds were taken at 300 and 4.2 K (Figs. 1 and 2). Owing to the large neutron-absorption cross section of dysprosium, a flat aluminum sample holder 0.2 cm thick was used. The 300-K patterns agree with the reported^{2,3} crystallographic structures. The lattice parameters are $a = b = 3.885 \text{ \AA}$, $c = 9.748 \text{ \AA}$ and $a = b = 3.964 \text{ \AA}$, $c = 9.982 \text{ \AA}$ for DyCo₂Si₂ and DyCu₂Si₂, respectively.

The 4.2-K pattern of DyCo₂Si₂ can be indexed according to a unit cell with $a = b = 3.872 \text{ \AA}$, $c = 9.669 \text{ \AA}$. However, additional reflections with $h + k + l = 2n + 1$, which are forbidden by the space group $I4/mmm$, appear. The peak intensity versus temperature of the lines $\{010\}$ and $\{111\}$ (Fig. 3) indicate a transition temperature at $21 \pm 2 \text{ K}$. The 4.2-K pattern of DyCu₂Si₂ differs from that of DyCo₂Si₂ and reveals the existence of superlattice lines. The pattern can be indexed with the lattice

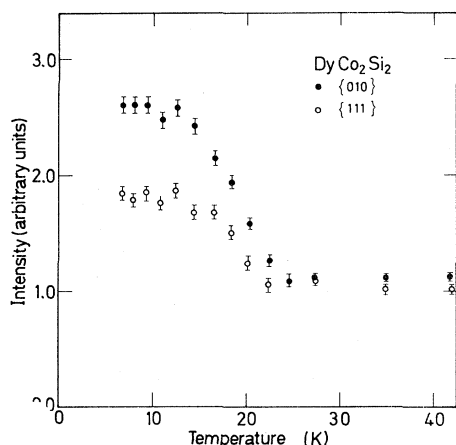


FIG. 3. Peak intensities of $\{010\}$ and $\{111\}$ vs temperature for DyCo₂Si₂.

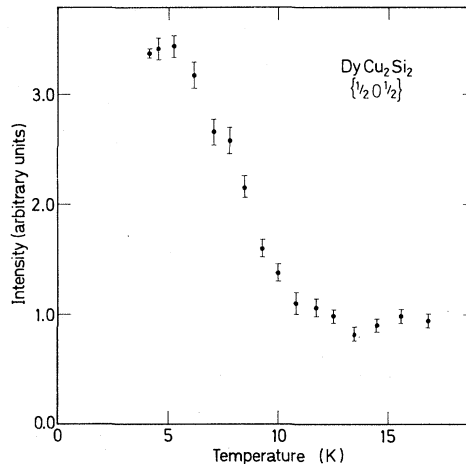


FIG. 4. Peak intensity of $\{\frac{1}{2}0\frac{1}{2}\}$ vs temperature for DyCu₂Si₂.

constants $a = b = 3.95 \text{ \AA}$, $c = 9.953 \text{ \AA}$ and superlattice lines where h and l equal half integers only. Hence the chemical cell is doubled in the a and c directions. The peak intensity of the line $\{\frac{1}{2}0\frac{1}{2}\}$ (Fig. 4) indicates a transition temperature at $11 \pm 1 \text{ K}$.

III. CRYSTALLOGRAPHIC STRUCTURES

The nuclear intensities were calculated for the structure shown in Fig. 5. The z parameter of Si and the absorption factor D were calculated to give a best fit with the observed integrated intensities (Table I). Owing to the large neutron-absorption cross section of dysprosium the refinement is not sensitive enough to changes in the Debye-Waller factor B . Compounds of the same family exhibit

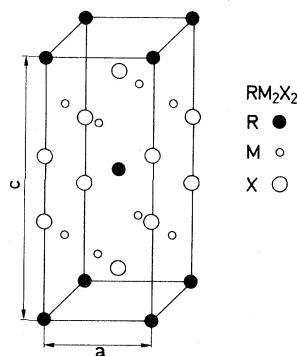


FIG. 5. Crystallographic structure of the RM₂X₂ family of compounds.

TABLE I. Comparison of calculated and observed integrated intensities in the 300 K patterns of DyCo₂Si₂ and DyCu₂Si₂. The calculated intensities were obtained with the use of the refined parameter values of Table II.

{hkl}	DyCo ₂ Si ₂		DyCu ₂ Si ₂	
	<i>I</i> _{obs} ± σ	<i>I</i> _{calc}	<i>I</i> _{obs} ± σ	<i>I</i> _{calc}
002	830 ± 120	940	150 ± 120	40
011	1950 ± 120	1700	1420 ± 120	1300
110	1640 ± 120	1590	420 ± 120	330
013	3130 ± 150	3280	2420 ± 150	2470
004	400 ± 150	310	400 ± 120	710
112	2970 ± 150	3170	5200 ± 150	5160
020	1890 ± 200	1710	2200 ± 400	2320
114 022	730 ± 200	430	120 ± 120	120
015 121	2110 ± 200	2000	1600 ± 260	1660

values such as 0 ± 0.4 Å² (Refs. 8 and 11), 0.4 ± 0.4 Å² (Ref. 8), and 0.9 ± 0.9 Å² (Ref. 9). We therefore assumed that *B* = 0 throughout the refinement. The refined parameters are given in Table II.

IV. MAGNETIC STRUCTURES

A. 4.2-K pattern of DyCo₂Si₂

In the 4.2-K pattern of DyCo₂Si₂ reflections with $h + k + l = 2n + 1$ (absent at 300 K) are present, with {00*l*} reflections missing. This result is consistent with a magnetic structure where $(\frac{1}{2}, \frac{1}{2}, \frac{1}{2})$ is an antitranlation and the magnetic axis is along *c*. It can be shown that the four possible configurations of the ordered Co sublattice will contribute to reflections with $h + k$ of single parity. The observed reflections, however, have $h + k$ of the two parities. Hence ordering of the dysprosium sublattice is necessary to explain the complete spectrum. The intensities were calculated for the structure where only the dysprosium sublattice is ordered

[Fig. 6(a)]. The *z* parameter of Si, the magnetic moment of dysprosium, and the absorption factor *D* were calculated to give a best fit to the observed integrated intensities. The calculated intensities and the observed integrated intensities are given in Table III. The possibility of simultaneous ordering of the dysprosium and cobalt sublattices was not considered.

B. 4.2-K pattern of DyCu₂Si₂

In the 4.2-K pattern of DyCu₂Si₂ the superlattice reflections are the following:

$$\left\{ \frac{1}{2} 0 \frac{1}{2} \right\}, \left\{ \frac{1}{2} 0 \frac{3}{2} \right\}, \left\{ \frac{1}{2} 0 \frac{5}{2} \right\}, \left\{ \frac{1}{2} 1 \frac{1}{2} \right\}, \\ \left\{ \frac{1}{2} 1 \frac{3}{2} \right\}, \left\{ \frac{1}{2} 0 \frac{7}{2} \right\}, \left\{ \frac{1}{2} 1 \frac{5}{2} \right\}, \left\{ \frac{3}{2} 0 \frac{1}{2} \right\}$$

(Fig. 2). The largest unit cell which can be made consistent with this set of reflections is $2a \times 2a \times 2c$. According to the Lifshitz condition¹⁵ in the theory of phase transitions of the second order only nine magnetic lattices are allowed below *T_N*. Eight of

TABLE II. Ionic parameters of DyCo₂Si₂ and DyCu₂Si₂ at 300 and 4.2 K.

Temperature (K)	Ion	μ(Dy) (μ _B)	C(Dy) ^a (Å ²)	<i>D</i> ^b	<i>z</i> (Si)	<i>R</i> ^c (%)
300	Co			2.46 ± 0.03	0.380 ± 0.004	9.1
	Cu			2.48 ± 0.03	0.384 ± 0.004	7.5
4.2	Co	9.5 ± 0.4	3.83	2.5 ± 0.5	0.37 ± 0.01	10.9
	Cu	8.3 ± 0.4	3.83	2.6 ± 0.5	0.38 ± 0.01	9.8

^aNot refined (see text).

^bAbsorption correction, $\exp(-D/\cos\theta)$, *D* = 2.5 corresponds to an effective thickness of 0.16 cm.

$$^c R = 100 \left[\frac{\sum [(I_{\text{obs}} - I_{\text{calc}})/\sigma]^2}{\sum (I_{\text{obs}}/\sigma)^2} \right]^{1/2}.$$

TABLE III. Comparison of calculated and observed integrated intensities in the 4.2-K pattern of DyCo_2Si_2 . The calculated intensities were obtained with the use of the refined parameter values of Table II.

$\{hkl\}$	$I_{\text{obs}} \pm \sigma$	I_{calc}
002	930±150	800
010	5050±200	4760
011	2170±200	1730
012	3130±200	3200
110	1330±230	1540
111	2740±230	3360
013 004 112	6180±280	6570
020 021	3480±280	2870
114 022	260±280	370
015 120 121	2770±280	2660

these lattices are shown in Fig. 7. The ninth lattice (not shown) is the body-centered tetragonal (bct) which prevails above T_N . Of these nine lattices only (3), (5), (6), and (8) will yield reflections at the observed positions. Among these only (3) represents a collinear structure where all the ions of the same sublattice have magnetic moments of the same magnitude. The corresponding orthogonal unit cell is $2a \times a \times 2c$. Assuming ordering of the copper sublattice only will result in a magnetic moment for the copper ion, much greater than the free-ion value. Therefore, we conclude that the dysprosium sublattice is ordered. A good fit of the calculated intensities to the observed integrated intensities (Table IV) is obtained with the use of lattice (3), and assuming that only the dysprosium sublattice is ordered with the magnetic axis along b . The magnetic structure is given in Fig. 6(b). The possibility of simultaneous ordering of the dysprosium and copper sublattices was not considered.

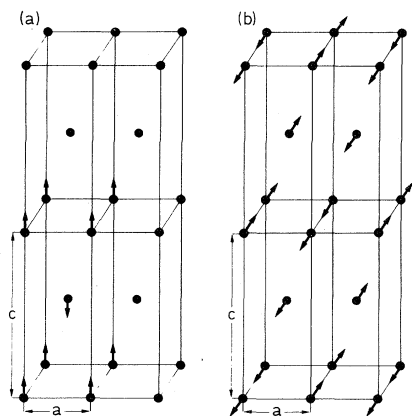


FIG. 6. Magnetic structure. (a) DyCo_2Si_2 , magnetic unit cell $a \times a \times c$. (b) DyCu_2Si_2 , magnetic unit cell $2a \times a \times 2c$.

TABLE IV. Comparison of calculated and observed integrated intensities in the 4.2-K pattern of DyCu_2Si_2 . The calculated intensities were obtained with the use of the refined parameter values of Table II.

$\{hkl\}$	$I_{\text{obs}} \pm \sigma$	I_{calc}
$\frac{1}{2}0\frac{1}{2}$	3240±150	3080
$\frac{1}{2}0\frac{3}{2}$ 002	1220±150	1420
101 011	700±120	700
$\frac{1}{2}0\frac{5}{2}$ $\frac{1}{2}1\frac{1}{2}$	770±150	890
$\frac{1}{2}1\frac{3}{2}$	360±130	340
110	160±120	180
$\frac{1}{2}0\frac{7}{2}$ $\frac{1}{2}1\frac{5}{2}$ $\frac{3}{2}0\frac{1}{2}$	770±240	900
103 013	1220±200	1330
004	280±280	380
$\frac{3}{2}0\frac{3}{2}$ 112	2880±250	2980
$\frac{1}{2}1\frac{7}{2}$ $\frac{3}{2}0\frac{5}{2}$ $\frac{3}{2}1\frac{1}{2}$	420±220	620
$\frac{1}{2}0\frac{9}{2}$	210±210	150
$\frac{3}{2}1\frac{3}{2}$	210±210	200
200 020	1320±120	1220
$\frac{3}{2}0\frac{7}{2}$	120±120	100
$\frac{3}{2}1\frac{5}{2}$	120±120	160
$\frac{1}{2}2\frac{1}{2}$	120±120	10
$\frac{1}{2}1\frac{9}{2}$	120±120	140
114	120±120	50
$\frac{1}{2}2\frac{3}{2}$	120±120	20
202 022	120±120	10

tices was not considered.

Magnetic form factor f and absorption factor D are highly correlated in the best-fit refinement. In the two compounds we therefore used $C=3.83 \text{ \AA}^2$ in the approximation $f=\exp(-C \sin^2\theta/\lambda^2)$ for the form factor which is consistent with the values calculated by Freeman and Watson¹⁶ for the dysprosium ion. The refined parameters are given in Table II.

A second method, in which the requirement that the transition is of second order had been relaxed, was used to solve the magnetic structure of DyCu_2Si_2 . A $2a \times 2a \times 2c$ unit cell was chosen containing 16 "independent" spins, half of which are opposite to the other half. Structure factors were calculated for all possible configurations $\frac{1}{2}\binom{16}{8}=6435$. There are many structures which yield the observed lines. However, only the structure shown in Fig. 6(b) results in a moment $gJ \sim 8.5\mu_B$, whereas any other structure will require

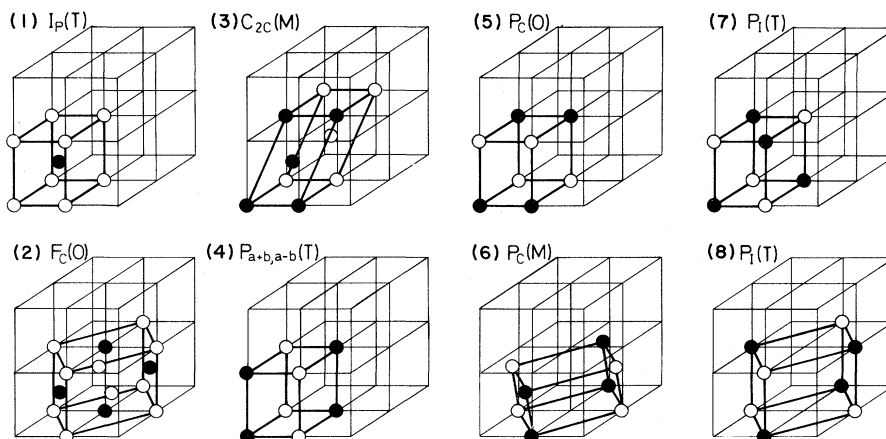


FIG. 7. The eight possible magnetic lattices allowed by the Lifshitz condition below T_N with their lattice designation (Ref. 19). Tetragonal, orthorhombic, and monoclinic lattices are indicated by T , O , and M , respectively.

that gJ be at least two times larger (i.e., $17\mu_B$), and is therefore unacceptable.

V. DISCUSSION

It was found that the Dy sublattice in DyCo_2Si_2 and DyCu_2Si_2 orders antiferromagnetically at low temperature. The Co compound orders with $(0,0,2\pi/c)$ as a propagation vector, hence preserving the chemical cell in the ordered state. The Cu compound, on the other hand, orders with $(\pi/a,0,\pi/c)$ as a propagation vector, quadrupling the volume of the chemical unit cell upon ordering. The magnetic structure found in the Co compound had been

found also in the germanides RCo_2Ge_2 , with $R=\text{Tb}$ and Ho . It is reasonable to expect then, that this structure will be found in the Tb and Ho silicides. Does this mean that the other structure is characteristic of the Cu compounds?

The dominant magnetic interaction in rare-earth transition-metal intermetallics is often of the Ruderman-Kittel type.¹⁷ With this interaction in compounds with heavy rare earths the transition temperatures follow the de Gennes function, that is, $T_N = C(g-1)^2J(J+1)$, where C is a molecular field constant independent of the rare earth.¹⁷ Observed T_N 's in three groups of RM_2X_2 intermetallics are fitted to this relation (Fig. 8) and a good agreement is found. The C values found in this way are about 1–4 K as compared to 20 K found for the rare-earth metals.¹⁷ On the basis of the agreement found so far, it is probably safe to predict that all RM_2X_2 with $R=\text{Gd}, \text{Tb}, \text{Dy}, \text{Ho}$, $M=\text{Co}, \text{Cu}$, and

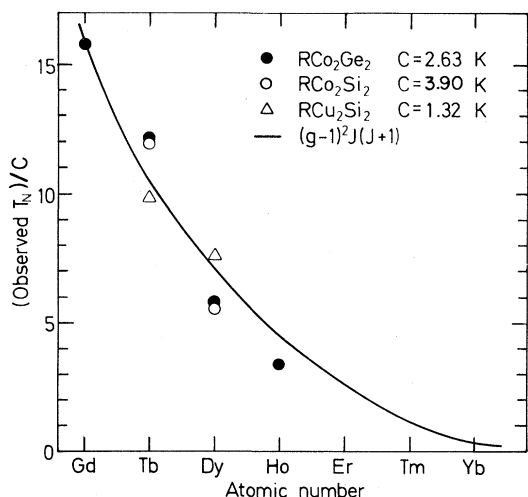


FIG. 8. Observed Néel temperatures of three groups of RM_2X_2 intermetallics and their relation to the de Gennes function.

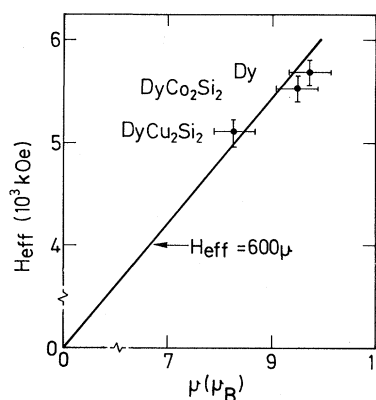


FIG. 9. Effective hyperfine magnetic fields in ^{161}Dy vs ordered magnetic moments.

$X=Si,Ge$ order antiferromagnetically at low temperatures. Erbium compounds, if they order, will order at very low temperatures.

There is the question of possible ordering of the M sublattice (in addition to the ordering found on the R sublattice). Only a small magnetic moment can be consistent with the neutron-diffraction results,^{1,11} which are in turn insensitive to such a small moment. The Mössbauer-effect studies of the ⁵⁷Fe (14-keV γ ray) in $DyFe_2Si_2$ and $DyFe_{0.5}Co_{1.5}Si_2$ indicate that the M sublattice is not ordered magnetically at low temperatures.¹² Hence, the absence of magnetic order on the M sublattice at $T < T_N$ is consistent with both the neutron-diffraction and the Mössbauer-effect data.

The effective hyperfine magnetic fields (H_{eff}) in $DyCu_2Si_2$, $DyCo_2Si_2$, and Dy metal as observed¹² in the Mössbauer effect in ¹⁶¹Dy are 5053, 5522, and

5681 kOe, respectively. The respective magnitudes of the ordered magnetic moment (μ) as observed in the neutron diffraction, are 8.3, 9.5 (Table II), and $9.8\mu_B$.¹⁸ These results yield (Fig. 9) H_{eff} (kOe) $\sim 600\mu$ (μ_B). The intensity temperature curves (Figs. 3 and 4) are not sharp and lead to Brillouin-type magnetization curves. This satisfies a necessary condition for a second-order transition.

ACKNOWLEDGMENTS

The authors are indebted to Mr. S. Fredo for preparation of the samples and to Mr. H. Ettegui for his technical aid. The authors wish to thank the Ministry of Science and Technology (BMFT), the Nuclear Research Establishment (RFA) of the Federal Republic of Germany, and the National Council for Research and Development (NRCD) of Israel for their partial support of this work.

¹Z. Ban and M. Sikirica, *Acta Crystallogr.* **18**, 594 (1965).

²D. Rossi, R. Marazza, and R. Ferro, *J. Less-Common Met.* **58**, 203 (1978).

³W. Rieger and E. Parthé, *Monatsh. für Chem.* **100**, 444 (1969).

⁴L. Omejec and Z. Ban, *Z. Anorg. Allg. Chem.* **380**, 111 (1971).

⁵I. Mayer, J. Cohen, and I. Felner, *J. Less Common Met.* **30**, 181 (1973).

⁶N. M. McCall, K. S. V. L. Narasimhan, and R. A. Butera, *J. Appl. Phys.* **44**, 4724 (1973).

⁷A. Szytula, J. Leciejewicz, and H. Bińczycka, *Phys. Status Solidi A* **58**, 67 (1980).

⁸H. Pinto and H. Shaked, *Phys. Rev. B* **7**, 3261 (1973).

⁹H. Pinto, M. Melamud, and E. Gurewitz, *Acta Crystallogr. Sect. A* **35**, 533 (1979).

¹⁰C. H. de Novion, J. Gal, and J. L. Buevoz, *J. Magn. Mater.* **21**, 85 (1980).

¹¹H. Pinto, M. Melamud, and H. Shaked, in *Symposium on Neutron Scattering—1981 (Argonne, Illinois)* (AIP, New York, in press).

¹²E. A. Görlich, Ph.D. thesis, Institute for Radiospectroscopy and Physics, Jagiellonian University, Cracow, Poland (1981).

¹³J. Leciejewicz, L. Chelmicki, and A. Zygmunt, *Solid State Commun.* **41**, 167 (1982).

¹⁴K. S. V. L. Narasimhan, V. U. S. Rao, W. E. Wallace, and I. Pop, in *Magnetism and Magnetic Materials—1975 (Philadelphia)*, Proceedings of the 21st Annual Conference on Magnetism and Magnetic Materials, edited by J. J. Becker, G. H. Lander, and J. J. Rhyne (AIP, New York, 1976), p. 594.

¹⁵E. M. Lifshitz, *J. Phys. (Moscow)* **VI**, 61 (1942).

¹⁶A. J. Freeman and R. E. Watson, *Acta Crystallogr.* **14**, 231 (1961).

¹⁷C. Kittel, *Quantum Theory of Solids* (Wiley, New York, 1963), p. 360.

¹⁸M. K. Wilkinson, W. C. Koehler, E. O. Wollan, and J. W. Cable, *J. Appl. Phys.* **32**, 48s (1961).

¹⁹W. Opechowski and R. Guccione, *Magnetism IIA*, edited by G. T. Rado and H. Suhl (Academic, New York, 1965), p. 105.